Homogeneous nucleation near a second phase transition and Ostwald's step rule

Z. Tavassoli [1] and R. P. Sear [2]

Department of Physics, University of Surrey, Guildford, Surrey, GU2 7XH, U.K.

Abstract

Homogeneous nucleation of the new phase of one transition near a second phase transition is considered. The system has two phase transitions, we study the nucleation of the new phase of one of these transitions under conditions such that we are near or at the second phase transition. The second transition is an Ising-like transition and lies within the coexistence region of the first transition. It effects the formation of the new phase in two ways. The first is by reducing the nucleation barrier to direct nucleation. The second is by the system undergoing the second transition and transforming to a state in which the barrier to nucleation is greatly reduced. The second way occurs when the barrier to undergoing the second phase transition is less than that of the first phase transition, and is in accordance with Ostwald's rule.

1 Introduction

The formation of a new phase at a first-order phase transition is an activated process. A nucleus of the new phase must overcome a free energy barrier in order to form and then grow into the new phase. The rate at which such microscopic nuclei form is proportional to $\exp(-\Delta F^*/kT)$, where ΔF^* is the height of the free energy barrier which the nuclei must overcome [1]. Here we consider nucleation of the new phase at a first-order phase transition and calculate ΔF^* when the system is near a second phase transition. One of the examples of nucleation near a second transition is nucleation of a crystalline phase at a first-order fluid-crystal transition near a fluid-fluid phase transition. Such a process has been observed in globular proteins whose phase diagrams show a metastable fluid-fluid transition within a strongly first-order fluid-crystal transition [2, 3]. Crystallisation of globular proteins is the subject of interest as protein crystals are needed in order to study their structure by X-ray diffraction [4–6]. It has been seen that globular proteins crystallize at temperatures near where we expect a metastable fluid-fluid critical point [7, 8]. Numerical work on nucleation near a critical point has been done by Talanquer and Oxtoby [9], where they obtained nuclei with very large numbers of molecules near the critical point. This followed pioneering computer simulations of ten Wolde and Frenkel [10], who found an anomalously low ΔF^* for the nucleation of a crystalline phase near the critical point of a metastable fluid-fluid transition. Other recent theoretical work on nucleation near a metastable transition may be found in [11–16] and references therein. Earlier theoretical work by one of us [14–16] showed that as the critical point is approached, the derivatives of the free energy barrier to nucleation with respect to the chemical potential and temperature diverge. Therefore the presence of the critical point causes a rapid drop in the free energy barrier to nucleation and so facilitates nucleation.

The metastable transition we consider here is an Ising-like or a vapour-liquid-like transition. An Ising-like transition is a transition from a phase with a negative magnetisation to a phase with a positive magnetisation. A vapour-liquid-like transition is a transition between two fluid phases differing in density. The metastable transition lies within the coexistence region of the equilibrium transition. Thus when the system is in the coexistence region of the metastable phase transition, it also lies within the coexistence region of the equilibrium transition. Then one of two new phases can nucleate: the stable phase can nucleate, as can the liquid phase or the analogue of the liquid phase, from the vapour phase or the analogue of the vapour phase. Which of these occurs first depends on which free energy barrier is lower. Thus the stable phase can be formed via two processes. In one process the free energy barrier to nucleation of the stable phase becomes small enough to allow nucleation, but the barrier to formation of the liquid phase is still large, then the stable phase nucleates. When the sizes of the barriers are reversed, then the formation of the stable phase occurs via two steps: first the liquid phase nucleates, and second the stable phase nucleates in this liquid phase.

Our finding that nucleation of a metastable transition can occur before nucleation of the stable phase, is just that observed by Ostwald more than 100 years ago [17, 18]. Ostwald's rule is that the phase that nucleates first is not necessarily the most thermodynamically stable phase, but is the one with closest free energy to the fluid phase. Later Stranski and Totomanow [19] improved this rule and suggested that the nucleated phase is the one with the lowest free energy barrier to nucleation, and not the phase that is globally stable.

Nucleation can be heterogeneous or homogeneous. In most circumstances suspended and dissolved impurities, as well as the solid boundaries provide sites for the formation of the new phase. This process is known as heterogeneous nucleation. However, in the absence of impurities or solid surfaces, small nuclei of the new phase are formed within the

[1] Electronic mail address: z.tavassoli@surrey.ac.uk
[2] Electronic mail address: r.sear@surrey.ac.uk

bulk of the system. This is a homogeneous nucleation and this is what we are studying here. A free energy barrier must be overcome in order to form nuclei of a critical size, beyond which the new phase grows spontaneously [1, 20]. The rate at which critical nuclei of the new phase are formed is very sensitive to the height of the free energy barrier. The so-called classical nucleation theory was originated with the work of Volmer and Weber [20,21] and originally developed for droplet condensation from supercooled vapours. The theory calculates the rate at which nuclei grow to a critical size, proportional to $\exp(-\Delta F_I^*/kT)$, where ΔF_I^* is the minimum work needed to form the critical nucleus.

In this paper we carry out numerical calculations to study the homogeneous nucleation of the new phase at a first-order transition near or at the second phase transition. The second transition is an Ising-like transition from the phase with a negative magnetisation to the phase with a positive magnetisation. In this work we use magnetic language, in fluid language the transition is from a low density phase to a high density phase. We present the results of numerical calculations for the temperatures below the critical point. The calculations are for the excess order parameter Δm^* and the free energy barrier to nucleation of the new stable phase, ΔF^*, in the critical nucleus. In the next section we study the theory of two types of homogeneous nucleation: nucleation of the new stable phase, and nucleation of the positive magnetisation phase from the negative magnetisation phase. We then discuss some of the numerical techniques we used in the calculations in section 3. In section 4 the results are presented and the last section is a conclusion.

2 Theory

2.1 Nucleation of a stable phase

We study nucleation of a new phase at a first-order transition near a second transition. The second transition is an Ising-like transition with an order parameter m. We work below the critical or Curie temperature and so we have a transition from negative m to positive m on increasing the field h. h is as usual the field which couples to m. Following earlier work by one of us [14] we split the nucleus of the new phase into two parts: the core and the fringe. That part of nucleus less than r_c from the origin is the core and the part farther than r_c is the fringe of the nucleus. We assume that the fringe of the nucleus is spherically symmetric. Therefore the order parameter $m(r)$ is a function only of r, the distance from the centre of the nucleus. As the universal behaviour of the nucleus is derived from the fringe, we therefore substitute the core by a boundary condition on $m(r)$ of the fringe. Thus for simplicity we fix $m(r \leq r_c) = m_c$, where the subscript c stands for the core of the nucleus. m_c is a positive constant independent of temperature and of h, and is essentially the value of the order parameter m in the nucleating phase. We require the excess free energy of the nucleus, ΔF, which is the free energy with a nucleus present minus that without a nucleus. Here we use a standard square-gradient functional for the fringe of the nucleus as a functional of the order parameter profile of the nucleus, $m(r)$, [1,22–24]

$$\Delta F = \Delta F_c + \int_{r>r_c} \left[\Delta\omega(m) + \kappa\left(\nabla m\right)^2\right] d\mathbf{r}, \tag{1}$$

where the first term is the contribution from the core of the nucleus, $\Delta F_c = \frac{4}{3}\pi r_c^3 \Delta\omega_{core}$, and the integral term is the contribution from the fringe of the nucleus. In Eq. (1) and all other equations, our free energies are in units of kT; k and T, Boltzmann's constant and the temperature, respectively. $\Delta\omega_{core}$ is a constant and is the excess free energy per unit volume of the core. As the core is close to the bulk equilibrium phase, $\Delta\omega_{core} < 0$ because the free energy is lower in the equilibrium phase. The gradient term in the integrand of Eq. (1) is due to the variations in space of $m(r)$. This is the lowest order term in a gradient expansion and is adequate when m is slowly varying. The coefficient κ is assumed to be a constant. In Eq. (1) $\Delta\omega$ in the integrand is given by

$$\Delta\omega = f(m) - f(m_b) - h(m - m_b), \tag{2}$$

where m_b is the order parameter in the bulk. $\Delta\omega$ is the work required per unit volume to change the order parameter from its bulk value m_b to m in the presence of an external field h. $f(m)$ is the bulk Helmholtz free energy per unit volume as a function of the order parameter $m(r)$. The critical nucleus is at the top of the free energy barrier and therefore at the maximum of ΔF. So we set the functional derivative of ΔF with respect to the order parameter profile $m(r)$, to zero,

$$\frac{\partial \Delta\omega(m)}{\partial m(r)} - 2\kappa\nabla^2 m(r) = 0, \quad r \geq r_c, \tag{3}$$

The total excess of the order parameter due to the presence of the nucleus, which is the total order parameter with the nucleus present minus that without the nucleus, is obtained as

$$\Delta m = \int (m(r) - m_b) d\mathbf{r}. \tag{4}$$

We employ Landau theory [25, 26] for the bulk free energy,

$$f(m,T) = \frac{1}{2} a t m^2 + b m^4, \tag{5}$$

where a and b are constants, and $t = T - T_c$ with T_c the critical temperature [26]. The bulk order parameter $m_b(h,T)$ is obtained by solving

$$\left.\frac{\partial \omega}{\partial m}\right|_{m=m_b} = 0, \tag{6}$$

where $\omega(m) = f(m) - hm$. Then using Eqs. (5,6) gives

$$atm + 4bm^3 - h = 0. \tag{7}$$

When $h = 0$ the bulk order parameter is that at coexistence and we call it m_{co}. For $h = 0$, Eq. (7) has just one real solution $m_{co} = 0$ for $T > T_c$. For $h = 0$ and $T < T_c$, Eq. (7) has three solutions, and consequently the free energy has two minima with the same free energy at $m_{co} = \pm\frac{1}{2}\left(-at/b\right)^{1/2}$, and a maximum at $m = 0$. In the presence of an external field h, Eq. (7) has one real solution for $T > T_c$, which corresponds to a single minimum for $\omega(m)$. When $T < T_c$ and $h \neq 0$ with $|h|$ not too large, there are two inequivalent minima in $\omega(m)$. For a fixed h, the absolute minimum corresponds to the equilibrium state and the higher minimum is a metastable state.

To get the order parameter profile we substitute Eq. (5) in Eq. (3), which gives

$$\frac{d^2 m}{dr^2} + \frac{2}{r}\frac{dm}{dr} - \frac{1}{2\kappa}\left(4bm^3 + atm - h\right) = 0, \tag{8}$$

for $r > r_c$, subject to boundary conditions

$$m(r = r_c) = m_c \tag{9}$$

and

$$m(r \to \infty) = m_b. \tag{10}$$

The former is the order parameter at the boundary between the fringe and the core, and the latter is the obvious condition that m tends towards its bulk value far from the nucleus. Eq. (8) is a nonlinear second-order differential equation which can not be solved analytically. We therefore use numerical methods to solve Eq. (8) for the order parameter profile, and then substitute it in Eq. (1) to obtain the excess free energy of the nucleus. The barrier to nucleation is at the maximum of the excess free energy and so will occur at a radius r_c^* given by $\partial\Delta F/\partial r_c = 0$. Thus we need to use a maximization method numerically to find r_c^* and hence ΔF^*, which is the free energy barrier to nucleation for a critical nucleus. This also gives $m^*(r)$ which is the order parameter profile of the critical nucleus. Substituting this profile in Eq. (4) we then find the excess order parameter of the critical nucleus Δm^*.

2.2 Nucleation of $+m$ phase from $-m$ phase, Classical Nucleation Theory

Starting in the $-m$ phase and increasing m (or equivalently h), we cross the phase transition from the $-m$ to the $+m$ phase. Then our system can not only nucleate the equilibrium phase but also the $+m$ phase. Then we are within both the $-m$ to $+m$ coexistence region and the coexistence region between the equilibrium phases. The nucleus of the $+m$ phase must overcome a free energy barrier in order to form, and then it grows to the new phase. The free energy barrier to form such critical nucleus is given by

$$\Delta F_I^* = \frac{16\pi\sigma^3}{3h^2}, \tag{11}$$

which is the standard classical nucleation theory expression [1, 26, 27]. This expression is valid for nucleation not too close to the spinodal [28]. The subscript I indicates that the transition is an Ising-like phase transition. In Eq. (11) σ is the surface free energy of the equilibrium interface between $+m$ and $-m$ phases, and is given by

$$\sigma = 2\int_{-m_{co}}^{m_{co}} \sqrt{\kappa\Delta f(m)}dm, \tag{12}$$

where $\Delta f(m) = f(m) - f(m_b)$ is the excess bulk free energy, Eq. (5).

It is worth mentioning that in this paper we have used a magnetic rather than a fluid language to describe the phase transitions. To switch from the magnetic language with a transition from $-m$ to $+m$ phase, to the fluid language with a vapour-liquid-like transition, the external field h becomes the chemical potential μ minus that at the coexistence μ_{co}, the order parameter m becomes density ρ, the bulk order parameters $-m_b$ and $+m_b$ become the vapour and liquid densities, ρ_v and ρ_l, respectively, and the axis $m = 0$ becomes the critical density $\rho_{cp} = (\rho_v + \rho_l)/2$ in the coexistence curve. Also in the fluid language the total order parameter Δm^* is equivalent to the total number of molecules in the critical nucleus.

3 Numerical Techniques

In the fringe far from the core, $m(r)$ is near the bulk order parameter m_b, we therefore use a Taylor expansion of $\Delta\omega(m)$ about $m = m_b$,

$$\Delta\omega(m) = \frac{1}{2}\chi^{-1}(m - m_b)^2 + \cdots \tag{13}$$

$$\frac{\partial\Delta\omega(m)}{\partial m} = \chi^{-1}(m - m_b) + \cdots, \tag{14}$$

where $\Delta\omega$ and its first derivative are zero at $m = m_b$. Here χ is the response function of m, defined by

$$\chi^{-1} = \left.\frac{\partial^2 f}{\partial m^2}\right|_{m=m_b}, \tag{15}$$

where $f(m)$ is the bulk free energy Eq. (5). Substituting Eq. (14) in Eq. (3) gives

$$\chi^{-1}(m - m_b) - 2\kappa\nabla^2(m - m_b) = 0, \tag{16}$$

which has a solution of Yukawa form

$$m(r) = m_b + B\,\frac{\exp(-r/\xi)}{r}, \tag{17}$$

for large values of r. To obtain Eq. (17) we used the boundary condition Eq. (10). In Eq. (17) B is a constant value which we will fix later, and ξ is the correlation length for $m(r)$ which is given by

$$\xi = (2\kappa\chi)^{1/2}. \tag{18}$$

The solution of $m(r)$ for large values of r has the form of Eq. (17). In numerical calculations we therefore use a large distance from the center of the core, R, to be the outer boundary of our numerical integration of Eq. (8), and use Eq. (17) beyond R.

For our numerical calculations we employ the Runge-Kutta method to solve the second-order differential Eq. (8) for the order parameter profile, subject to boundary conditions at r_c and R, Eq. (9) and Eq. (17), respectively. The

constant value B in Eq. (17) is then obtained by finding the root of the nonlinear equation $m(r_c) - m_c = 0$, for which we used Ridders' method [29]. Substituting the order parameter profile $m(r)$ in Eq. (1) gives the excess free energy of the nucleus. The barrier to nucleation is at a maximum of ΔF and so will occur at a radius r_c^* given by $\partial \Delta F / \partial r_c = 0$. We then use a maximization method to obtain r_c^* and consequently $m^*(r)$ and the barrier to nucleation ΔF^*.

In the numerical calculations we used a large radius R for the boundary condition of the fringe of the nucleus. We need such a value to enable us to carry out the numerical calculations. We calculate the contribution of distances larger than R analytically and add it to the corresponding numerical quantity for the range r_c to R, as a correction term. The correction term for the excess order parameter of the critical nucleus, Δm^*, can be calculated using Eq. (4) with the limits for the integral from R to ∞. Then by substituting Eq. (17) for $m(r)$ for all values of $r \geq R$, the correction term is

$$\Delta m_{ct}^* = 4\pi\kappa B\xi(R+\xi)e^{-R/\xi}, \tag{19}$$

where ct stands for the correction term. The correction term for the free energy barrier to nucleation ΔF^*, is calculated using the integral term in Eq. (1) for all values of r from R to ∞. Then by substituting Eq. (13) in $\Delta\omega(m)$ and using the normal gradient of Eq. (17) for $\nabla m(r)$, the correction term is given by

$$\Delta F_{ct}^* = 4\pi\kappa B^2 \left(\frac{1}{R} + \frac{1}{\xi}\right) e^{-2R/\xi}, \tag{20}$$

which we have used the definition of ξ, Eq. (18).

The solution of Eq. (17) for the order parameter for $r \geq R$ is derived using the Taylor expansion of $\Delta\omega(m)$ about $m = m_b$, Eq. (13). In this expansion we have used up to the second-order term of $(m - m_b)$ and have ignored the higher orders. We therefore need to obtain the conditions under which we are allowed to use this approximation. To do so we see that in Eq. (13) by ignoring terms of orders greater than 2, we have assumed that these values are less than the second-order term. The biggest of all ignored terms is the third order one, we have therefore assumed that

$$\left.\frac{\partial^3 \Delta\omega(m)}{\partial m^3}\right|_{m=m_b} \frac{(m-m_b)^3}{3!} \ll \frac{1}{2}\chi^{-1}(m-m_b)^2. \tag{21}$$

Using Eqs. (5,18) in Eq. (21) gives

$$\frac{4b}{\kappa} m_b \, \xi^2 (m(R) - m_b) \ll 1, \tag{22}$$

as the requirement that must be satisfied. Here $m(R)$ is given by Eq. (17) at $r = R$.

4 Results

The free energy barriers to nucleation of the stable phase and of the $+m$ phase are ΔF^* and ΔF_I^*, respectively. In each nucleation the formation of the new phase occurs when the free energy barrier is of roughly $30kT$. The figure $30kT$ is rather arbitrary [1] but the nucleation rate is of order, number of molecules times $\exp(-\Delta F^*/kT)$ divided by the characteristic time scale of the solution. The characteristic time scale of protein solutions is of order $1\mu s$ [3]. Thus a volume of the solution containing 10^9 protein molecules has a nucleation rate of order $10^9 \times e^{-30} \times 10^6 \approx 10 s^{-1}$. Thus in a volume of the solution containing a billion molecules, nuclei will appear in a fraction of a second. When the barrier reaches $30kT$ the $-m$ phase is unstable and the stable $+m$ phase nucleates immediately. A barrier of about twice this, $60kT$, is required for the $-m$ phase to be stable over long times, i.e., for it to be metastable. Homogeneous nucleation of a new stable phase near a second phase transition has been studied before [9–16]. Here we carried out numerical calculations for Δm^* and ΔF^*. Near the critical point the scaling of the size of the critical nucleus is [14–16],

$$\Delta m^* \sim |t|^{-\gamma} g_{\pm}\left(h/|t|^{\beta\delta}\right), \tag{23}$$

and that of the free energy is

$$\Delta F_s^* \sim |t|^{\beta} f_{\pm}\left(h/|t|^{\beta\delta}\right), \tag{24}$$

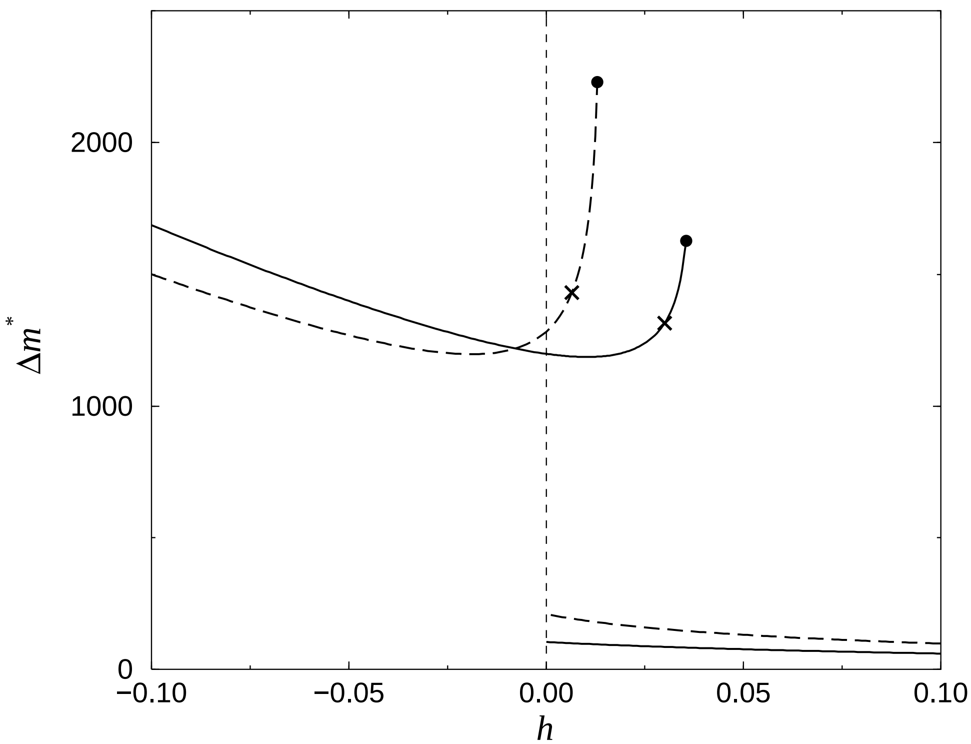

Figure 1: Δm^* versus h at two temperatures below the critical temperature, when $\kappa = 1$ and $\Delta\omega_{core} = -0.5$. Solid and long-dashed curves correspond to $t = -0.5$ and $t = -0.25$, respectively.

for both temperatures above and below the critical temperature. Here $\pm$ are related to $t > 0$ and $t < 0$, γ, β and δ are the usual critical exponents, and take values of 1, 1/2 and 3 within mean-field theory. In Eq. (24) subscript s stands for singular part of the fringe. These results were predicted in earlier work [14–16] and we confirmed them by numerical calculations. As the critical point is approached, the magnetisation of the critical nucleus Δm^* diverges, and so does the derivative of the free energy barrier to nucleation ΔF^*, with respect to the temperature and to h. We are also interested in the behaviour of Δm^* and ΔF^* far from the critical point.

4.1 Far from the critical point

Here we study the total magnetisation and the free energy of the critical nucleus, Δm^* and ΔF^*, respectively, far from the critical point — $|t|$ not small. In all the calculations we have fixed $a = b = m_c = 1$. In Figs. 1 and 2 there are graphs of Δm^* and ΔF^*, respectively, for two different temperatures below and far from the critical temperature, $t = -0.25$ and $t = -0.5$ with $\kappa = 1$ and $\Delta\omega_{core} = -0.5$. For each temperature, when $h < 0$ the system is in a state with a negative order parameter $m < 0$ less than that at the coexistence. When $h > 0$ the system can be found in a state with a positive order parameter $m > 0$ greater than that at the coexistence. For $h > 0$ there are also states with $m < 0$ between the $-m$ branch of the coexistence curve and the spinodal. These states are within two coexistence regions: the coexistence region between $-m$ and $+m$ phases, and that between the equilibrium phases. Therefore in both Figs. 1 and 2, for each temperature there are values of $h > 0$ for which Δm^* and ΔF^* are double valued. These values correspond to the $-m$ phase between the coexistence and spinodal curves, and the $+m$ phase with a lower Δm^* and ΔF^*.

In Fig. 1 for each temperature as h increases the curves on the right-hand side decrease. Those on the left-hand side decrease first and then increase rapidly. Decreasing Δm^* is due to the fact that for a higher h, the bulk order parameter m_b is higher and thus it leads to a lower excess order parameter Δm^* in Eq. (4). However the large and rapidly increasing values of Δm^* are due to the proximity to the spinodal. As we approach the spinodal the response function of the order parameter, χ defined as in Eq. (15) diverges. Therefore the total excess order parameter Δm^* which scales as χ [14–16] will diverge as well. As the temperature approaches T_c ($|t|$ decreases), Δm^* diverges at a lower value of h. This is because, as T approaches T_c, the gap between the coexistence and the spinodal curves decreases. In Fig. 2 for each temperature as h increases ΔF^* decreases, due to the increase in the bulk order parameter m_b. The phase with the higher order parameter must overcome a lower free energy barrier ΔF^* to form a nucleus of the equilibrium phase, whose order parameter we have set equal to 1. Also in Fig. 2, ΔF^* varies rapidly as it approaches the spinodal.

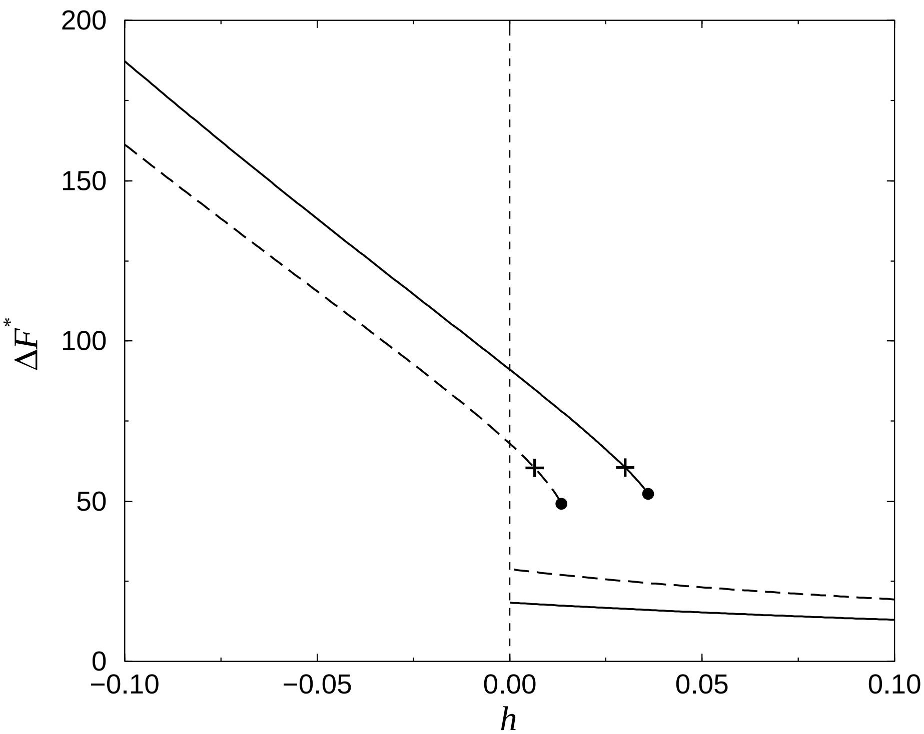

Figure 2: ΔF^* versus h for two different temperatures, when $\kappa = 1$ and $\Delta\omega_{core} = -0.5$. Solid and long-dashed curves correspond to $t = -0.5$ and $t = -0.25$, respectively.

This is due to what is called the nucleation theorem [30–32] and states that the derivative of the free energy barrier with respect to h is equal to minus the excess m, $\partial\Delta F^*/\partial h = -\Delta m^*$ [14–16]. It shows that the larger Δm^* is, the more rapidly the free energy barrier varies with h. As the spinodal is approached Δm^* diverges and thus ΔF^* drops rapidly with h. When a transition from $-m$ to $+m$ phase occurs both Δm^* and ΔF^* in Figs. 1 and 2 jump to lower values, because of the increase in m_b. The height of this reduction is temperature-dependent because the bulk order parameters $m_{co} = \pm\sqrt{(-t/4)}$ are functions of $t = T - T_c$. As the temperature decreases, the difference between these two order parameters increases, and therefore the height of the drop in both Δm^* and ΔF^* increases.

For each temperature as h increases ΔF_I^* decreases, Eq. (11), and for energy barriers of about $30kT$ a transition of $-m$ phase to $+m$ phase with lower values of Δm^* and ΔF^* occurs. The cross marks on the graphs in Figs. 1 and 2 are the points where $\Delta F_I^* = 30kT$. Also in the region with $h > 0$ and $m < 0$ the solutions to Δm^* and ΔF^* disappear at a value of h before the spinodal. The circle marks on the graphs are the points for which the solutions disappear. For this value of h in our numerical calculations the solution to the order parameter profile of the critical nucleus, $m^*(r)$, disappears. The solution to $m^*(r)$ is obtained by solving Eq. (3) subject to the boundary condition $m^*(r = r_c^*) = m_c$. In the region between the $-m$ branch of the coexistence and the spinodal with $h > 0$, Eq. (3) gives two solutions for $m^*(r)$, out of which we choose the one with lower free energy barrier, ΔF^*. As h increases, these two solutions approach each other until they become equal at a specific value of $h > 0$. For any value of h greater than this, then there is no solution. This means that the critical nucleus does not exist anymore and there is no well defined free energy barrier to nucleation. As we see in Figs. 1 and 2 for each temperature the points with $\Delta F_I^* = 30kT$ (cross marks) are at the left side of those for which the solutions disappear (circle marks). As for energy barriers of $\Delta F_I^* = 30kT$ a transition of $-m$ to $+m$ phase occurs, therefore for these parameter values as the system approaches the cross marks, the $-m$ phase will transform to $+m$ phase. Thus in the experiments the states after the cross marks are not accessible. As we see in Figs. 1 and 2 as the temperature approaches T_c ($|t|$ decreases), the solution disappears at a lower value of $h > 0$. This is because as T approaches T_c, the coexistence and the spinodal curves approach each other.

The stable phase can be attained via two processes [33]. In one process ΔF^* drops below $30kT$ when ΔF_I^* is still large, then the stable phase is reached in one step through nucleating in $-m$ phase. In the second process ΔF_I^* drops below $30kT$ when ΔF^* is still large, then the stable phase will be reached in two steps: first the $+m$ phase nucleates in the $-m$ phase and grows and then second, the stable phase nucleates in this $+m$ phase. The fact that the nucleated phase is the one which has lower free energy barrier and not necessarily the stable phase, is in accordance with Ostwald's step rule. In Fig. 2 with $\Delta\omega_{core} = -0.5$ the barrier ΔF^* is always greater than $30kT$ when ΔF_I^* drops below $30kT$.

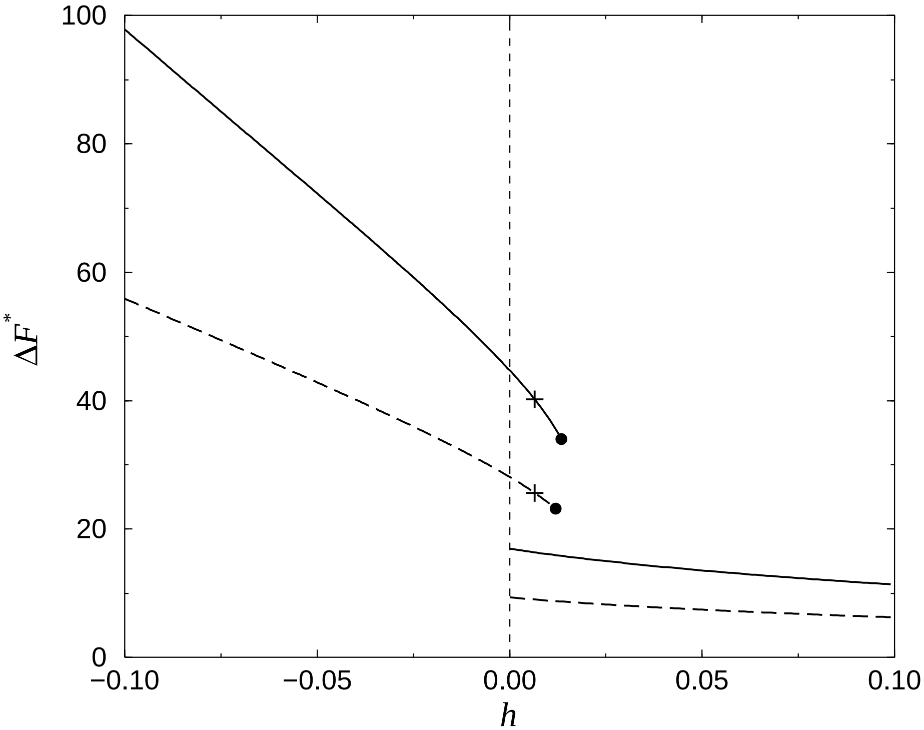

Figure 3: ΔF^* versus h for two $\Delta\omega_{core}$, when $\kappa = 1$ and $t = -0.25$. Solid and long-dashed curves correspond to $\Delta\omega_{core} = -0.75$ and $\Delta\omega_{core} = -1.25$, respectively.

Thus on increasing h the $+m$ phase nucleates before the equilibrium phase. The equilibrium phase then nucleates in the $+m$ phase. But as $\Delta\omega_{core} < 0$, when $\Delta\omega_{core}$ becomes more negative then ΔF_c^* becomes more negative and therefore ΔF^* in Eq. (1) drops. So for sufficiently negative values of $\Delta\omega_{core}$, ΔF^* drops below $30kT$ before ΔF_I^* does and the stable phase nucleates before the $+m$ phase. To show this, in Fig. 3 graphs of ΔF^* are plotted for two values of $\Delta\omega_{core} = -0.75$ and $\Delta\omega_{core} = -1.25$, when $t = -0.25$. Just as in the previous figures, the cross marks on each graph correspond to where $\Delta F_I^* = 30kT$ and the circle marks are where the solutions disappear. For $\Delta\omega_{core} = -0.75$, ΔF^* is greater than $30kT$ when ΔF_I^* drops below $30kT$. Thus the $+m$ phase nucleates first and then the equilibrium phase nucleates in the $+m$ phase. For $\Delta\omega_{core} = -1.25$ however ΔF^* drops below $30kT$ before ΔF_I^* does. Thus the equilibrium phase nucleates before the $+m$ phase. The values of h for which $\Delta F_I^* = 30kT$ (the cross marks) are independent of $\Delta\omega_{core}$ and are the same on both graphs. This is because ΔF_I^* in Eqs. (11,12) depends only on the temperature and on h, and is independent of $\Delta\omega_{core}$.

The two step route to the equilibrium phase that we find is not dissimilar to that proposed for the crystallisation of some polymer melts by Olmsted et. al. [34]. They study a system with the same phase diagram as considered here but their equivalent of the $-m$ to $+m$ phase transition proceeds via spinodal decomposition and not nucleation as here. Thus the results here apply to liquids and colloidal suspensions, where the new phase nucleates, whereas Olmsted et. al.'s approach is more applicable to polymers.

We are also interested to study where the free energy barrier $\Delta F_I^* = 30kT$, and a nucleation from the $-m$ phase to the $+m$ phase occurs. Up to now we considered systems with $\kappa = 1$. We also like to know the effect of increasing κ on the calculations. In Figs. 4 and 5 there are diagrams of t versus m, and t versus h, respectively for three different values of κ when $\Delta\omega_{core} = -0.5$. In Fig. 4 the solid (outermost) and long-dashed (innermost) curves represent the coexistence and the spinodal, respectively. The other curves in Fig. 4 between the coexistence and spinodal curves correspond to the points with energy barriers of $\Delta F_I^* = 30kT$ for different κ. From left to right, dotted, dashed and dot-dashed curves are for $\kappa = 1, 1.5$ and 2, respectively. In Fig. 5 the solid line $h = 0$ along axis t corresponds to coexistence, and the long-dashed curve (the outermost) represents spinodal. The other curves in Fig. 5 between the coexistence and the spinodal correspond to the points with $\Delta F_I^* = 30kT$ for different κ. From left to right, dotted, dashed and dot-dashed curves represents $\kappa = 1, 1.5$ and 2, respectively. As κ increases there is a shift towards larger values of both m and h for $\Delta F_I^* = 30kT$. This shift can be explained as follows. For a fixed temperature and external field h, a higher κ yields a higher free energy barrier to nucleation of the $+m$ phase ΔF_I^* (11,12). Now for each fixed temperature and κ, as h increases the energy barrier ΔF_I^*, Eq. (11), decreases until it reaches energies of about $30kT$. Therefore at each

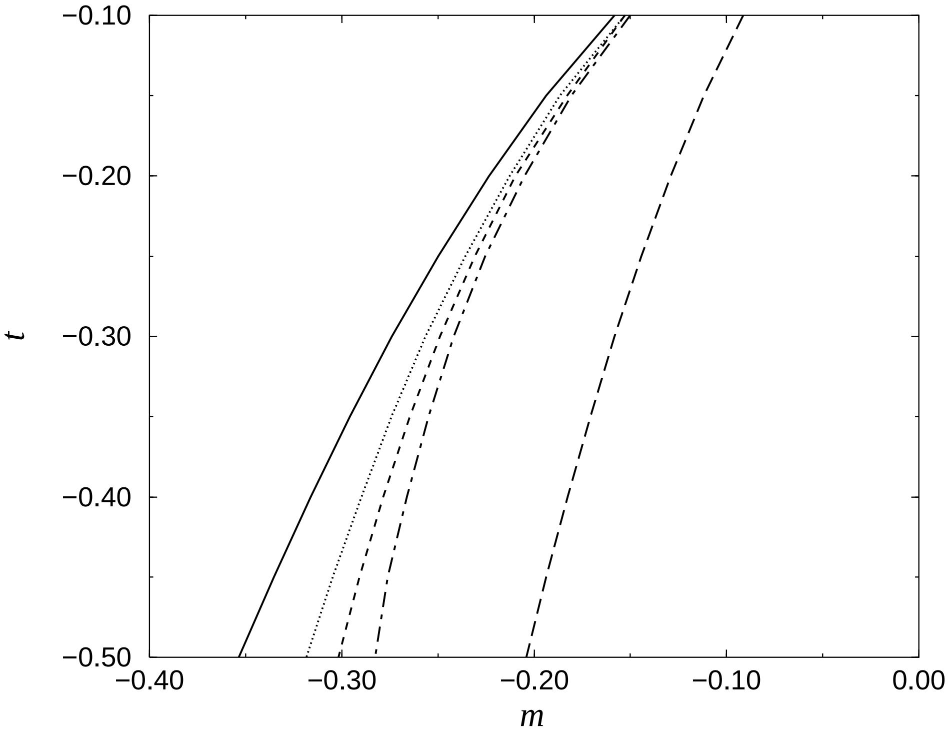

Figure 4: Phase diagram for t versus m. Solid and long-dashed lines are coexistence and spinodal, respectively. The others correspond to $\Delta F_I^* = 30kT$, dotted, dashed and dot-dashed lines are for $\kappa = 1, 1.5$ and 2, respectively.

fixed temperature, for a higher κ the nucleation occurs at a higher external field h and consequently at a higher order parameter m. Increasing κ also increases ΔF^* Eq. (1), thus increasing κ pushes nucleation to both the $+m$ and the stable phase to larger values of h.

5 Conclusions

Homogeneous nucleation of a new phase at a first-order transition near a second transition is considered. The second transition is an Ising-like or a vapour-liquid-like transition, and lies within the coexistence region of the equilibrium transition. Numerical calculations were performed to calculate the excess order parameter Δm^* and the free energy barrier to nucleation ΔF^*, of the critical nucleus. For the states in the negative magnetisation phase with $h > 0$ the system is within the coexistence regions of both transitions. Then in these states either the positive magnetisation phase or the equilibrium phase can nucleate. The free energy barriers to nucleation are equal to ΔF_I^* and ΔF^*, for the former and the latter, respectively. The phase which nucleates is the one with the lower free energy barrier. This is in accordance with Ostwald's step rule, which states that the nucleated phase is not necessarily the stable phase, but is the one with the lowest free energy barrier to nucleation. The stable phase can be attained via two processes. In the first process ΔF^* becomes small enough to allow nucleation when ΔF_I^* is still large, then the stable phase nucleates. In the second process ΔF_I^* becomes small enough to allow nucleation when ΔF^* is still large, then the stable phase will be reached in two steps: first the positive magnetisation phase nucleates and grows and then second, the stable phase nucleates in this positive magnetisation phase.

When the Ising-like phase transition occurs, both Δm^* and ΔF^* jump to lower values, due to the increase in the bulk order parameter. As the bulk order parameter at coexistence is a function of the temperature, then the height of the jump is temperature-dependent. For a lower temperature, the jump in the order parameter increases and therefore the jumps in Δm^* and the barrier to nucleation ΔF^* increase. This may mean a jump from a nucleation barrier too high to permit significant nucleation, to a very small barrier that results in rapid nucleation with many nuclei forming. This effect may cause problems for crystallographers wanting to achieve a small but non-zero rate of nucleation in order to obtain a few large crystals. We also observed that as the spinodal is approached, Δm^* diverges and the free energy barrier ΔF^* varies rapidly with h.

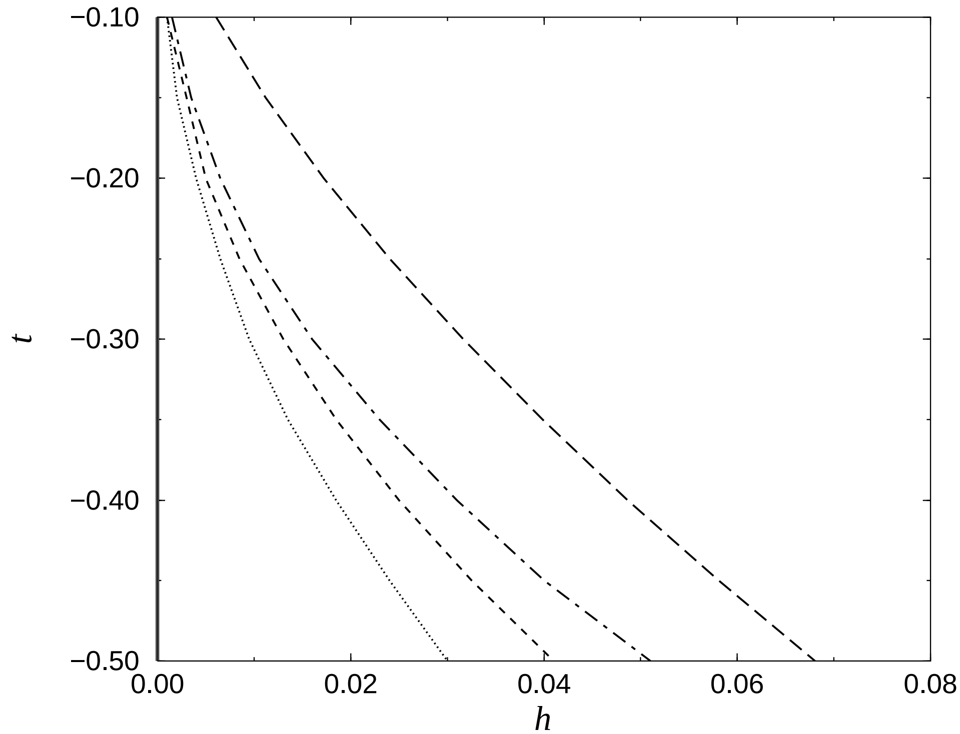

Figure 5: Phase diagram for t versus h. Coexistence lies along the t axis. Long-dashed curve is the spinodal. The others correspond to $\Delta F_I^* = 30kT$, dotted, dashed and dot-dashed lines are for $\kappa = 1, 1.5$ and 2, respectively.

Acknowledgements

This work is supported by EPSRC (GR/N36981).

References

[1] P. G. Debenedetti, *Metastable Liquids* (Princeton University Press, Princeton, 1996).

[2] M. L. Broide, C. R. Berland, J. Pande, O. O. Ogun and G. B. Benedek, Proc. Nat. Acad. Sci. **88**, 5660 (1991).

[3] M. Muschol and F. Rosenberger, J. Chem. Phys. **107**, 1953 (1997).

[4] F. Rosenberger, P. G. Vekilov, M. Muschol and B. R. Thomas, J. Crys. Growth **168**, 01 (1996).

[5] N. Chayen and J. Helliwell, Physics World, May **43** (1998).

[6] R. Piazza, Curr. Opin. Coll. Int. Sci. **5**, 38 (2000).

[7] A. George and W. Wilson, Acta Crystallogr. D **50**, 361 (1994).

[8] D. Rosenbaum, P. C. Zamora and C. F. Zukoski, Phys. Rev. Lett. **76**, 150 (1996).

[9] V. Talanquer and D. W. Oxtoby, J. Chem. Phys. **109**, 223 (1998).

[10] P. R. ten Wolde and D. Frenkel, Science **277**, 1975 (1997).

[11] C. Haas and J. Drenth, J. Phys. Chem. B **104**, 368 (2000).

[12] N. M. Dixit and C. F. Zukoski, J. Coll. Int. Sci. **228**, 359 (2000).

[13] D. Pini, G. Jialin, A. Parola and L. Reatto, Chem. Phys. Lett. **327**, 209 (2000).

[14] R. P. Sear, Phys. Rev. E **63**, 066105 (2001).

[15] R. P. Sear, J. Chem. Phys. **114**, 3170 (2001).

[16] R. P. Sear, submitted to J. Chem. Phys .

[17] W. Ostwald, Z. Phys. Chem. **22**, 289 (1897).

[18] P. R. ten Wolde and D. Frenkel, Phys. Chem. Chem. Phys. **1**, 2191 (1999).

[19] I. N. Stranski and D. Totomanow, Z. Phys. Chem. **163**, 399 (1933).

[20] F. F. Abraham, *Homogeneous Nucleation Theory. The Pretransition Theory of Vapor Condensation* (Academic Press, New York, 1974).

[21] M. Volmer and A. Weber, Z. Phys. Chem. **119**, 277 (1926).

[22] J. W. Cahn and J. E. Hilliard, J. Chem. Phys. **31**, 688 (1959).

[23] J. W. Cahn and J. E. Hilliard, J. Chem. Phys. **28**, 258 (1958).

[24] B. Widom, Chem. Soc. Rev. **14**, 121 (1985).

[25] L. P. Kadanoff, *Statistical Physics* (World Scientific, Singapore, 2000).

[26] P. M. Chaikin and T. C. Lubensky, *Principles of Condensed Matter Physics* (Cambridge University Press, Cambridge, 1995).

[27] L. D. Landau and E. M. Lifshitz, *Statistical Physics, Part 1*, vol. 5 of *Course of Theoretical Physics*, 3rd edn. (Pergamon Press Ltd., Oxford, 1980).

[28] K. Binder, Phys. Rev. A **29**, 341 (1984).

[29] W. H. Press, S. A. Teukolsky, W. T. Vetterling and B. P. Flannery, *Numerical Recipes in C* (Cambridge University Press, Cambridge, 1992).

[30] D. Kashchiev, J. Chem. Phys. **76**, 5098 (1982).

[31] Y. Viisanen, R. Strey and H. Reiss, J. Chem. Phys. **99**, 4680 (1993).

[32] R. K. Bowles, R. McGraw, P. Schaaf, B. Senger, J. C. Voegel and H. Reiss, J. Chem. Phys. **113**, 4524 (2000).

[33] W. C. K. Poon, F. Renth, R. M. L. Evans, D. J. Fairhurst, M. E. Cates and P. N. Pusey, Phys. Rev. Lett. **83**, 1239 (1999).

[34] P. D. Olmsted, W. C. K. Poon, T. C. B. Mcleish, N. J. Terrill and A. J. Ryan, Phys. Rev. Lett. **81**, 373 (1998).